

## Complete control of a matter qubit using a single picosecond laser pulse

Y. Kodriano,<sup>1</sup> I. Schwartz,<sup>1</sup> E. Poem,<sup>1</sup> Y. Benny,<sup>1</sup> R. Presman,<sup>1</sup> T. A. Truong,<sup>2</sup> P. M. Petroff,<sup>2</sup> and D. Gershoni<sup>1,\*</sup>

<sup>1</sup>*Department of Physics, The Technion–Israel Institute of Technology, Haifa, 32000, Israel*

<sup>2</sup>*Materials Department, University of California, Santa Barbara, California 93106, USA*

(Received 31 January 2012; published 13 June 2012)

We demonstrate that a matter physical two-level system, a qubit, can be fully controlled using one ultrafast step. We show that the spin state of an optically excited electron, an exciton, confined in a quantum dot, can be rotated by any desired angle, about any desired axis, during such a step. For this we use a single, resonantly tuned, picosecond long, polarized optical pulse. The polarization of the pulse defines the rotation axis, while the pulse detuning from a nondegenerate absorption resonance defines the magnitude of the rotation angle. We thereby achieve a high fidelity, universal gate operation, applicable to other spin systems, using only one short optical pulse. The operation duration equals the pulse temporal width, orders of magnitude shorter than the qubit evolution life and coherence times.

DOI: [10.1103/PhysRevB.85.241304](https://doi.org/10.1103/PhysRevB.85.241304)

PACS number(s): 78.67.Hc, 42.50.Dv, 02.30.Yy, 03.67.Lx

Matter qubits are essential for any realization of quantum information processing. Spins of particles are promising candidates for qubits, since nuclear, atomic, or electronic spins are natural, relatively protected, physical two-level systems. Their spin state can be described as a coherent superposition of the two levels and thereby geometrically as a vector pointing from the center of a unit sphere whose poles are formed by the two levels, to a point on the sphere surface (Bloch sphere). An important prerequisite for a qubit is the ability to fully control its state. A geometrical description of such a universal operation is a rotation of the qubit's state vector by any desired angle, about any desired axis.<sup>1,2</sup> Naturally, a universal operation should be performed with very high fidelity and completed within a very short time. The control time should be orders of magnitude shorter than the qubit's life and decoherence times.<sup>3</sup>

If the two spin eigenstates are nondegenerate (e.g., in a magnetic field), the spin state evolves in time. This evolution is described as a precession of the state vector about an axis connecting the sphere's poles, at a frequency which equals the energy difference between the two eigenstates divided by the Planck constant.

The control methods demonstrated thus far use a sequence of optical pulses, which induce fixed rotations of the qubit around axes which differ from the precession axis (Ramsey interference). A delay between the pulses allows the qubit to coherently precess between the pulses and thus a universal operation is achieved. Clearly, such a sequence of steps increases the time required to perform the operation, resulting in an operation time comparable to the precession period. Moreover, the operation fidelity equals the product of the fidelities of each step. In contrast, we demonstrate that a *single, picosecond*, optical pulse can be utilized to achieve complete control of a matter qubit, composed of an optically excited electron (exciton) in a *single semiconductor quantum dot*.<sup>4–9</sup> Our demonstration is by no means unique to this technologically important system and is applicable to other systems as well. We thereby provide a fast and efficient universal single-qubit gate, which has not been demonstrated previously in any other platform.

Spins of charge carriers in semiconductor quantum dots (QDs) are particularly important candidates for qubits<sup>10,11</sup>

since they dovetail with contemporary technologies and since they form an excellent interface between “flying” qubits (photons) and “anchored” qubits (spins). A few steps spin control in QDs was demonstrated by radio-frequency pulses<sup>12,13</sup> and by optical means using stimulated Raman scattering<sup>14–18</sup> or by accumulation of a “geometrical phase” through resonant excitation.<sup>19–24</sup>

The qubit discussed here is formed by resonant optical excitation of an electron from the highest energy full valence band to the lowest energy empty conduction band. Such excitation can be viewed as photogeneration of an electron–heavy-hole pair of opposite spins (bright exciton). Due to the reduced symmetry of the QD, the exchange interaction within the pair removes the degeneracy between its two possible spin configurations and forms symmetrical ( $|H\rangle$ ) and antisymmetrical ( $|V\rangle$ ) eigenstates, which upon recombination emit light polarized parallel to the major ( $H$ ) and minor ( $V$ ) axes of the QD, respectively (Fig. 1). It follows that any coherent superposition of these eigenstates, photogenerated by nonrectilinearly polarized light, precesses in time with a period  $T$ , inversely proportional to the energy difference between the two eigenstates.<sup>8</sup>

The control of the qubit is demonstrated by performing a series of experiments using sequences of three synchronized optical pulses as shown in Fig. 1(a). The first optical pulse is a polarized pulse which we tune to an excitonic absorption resonance. It photogenerates an exciton while translating the light polarization into exciton spin polarization, with high fidelity.<sup>8</sup> In order to probe (read) the exciton spin qubit's state, another picosecond pulse tuned into a two-exciton (biexciton) resonance<sup>8</sup> is used. This pulse photogenerates an additional electron-hole pair and transfers the excitonic population into a biexcitonic population.<sup>8,9,25</sup> The absorption of the probe pulse depends on the relative spin orientation of the two pairs. Since the probe polarization defines the spin of the second pair, its absorption measures the exciton's spin projection on its polarization direction.<sup>8,9,25</sup> The magnitude of the absorption is then directly deduced from the intensity of the photoluminescence (PL) of the biexciton emission lines<sup>25</sup> [Fig. 1(b)].

The ability to accurately prepare and probe an excitonic qubit<sup>8</sup> enables us, in turn, to demonstrate full control over

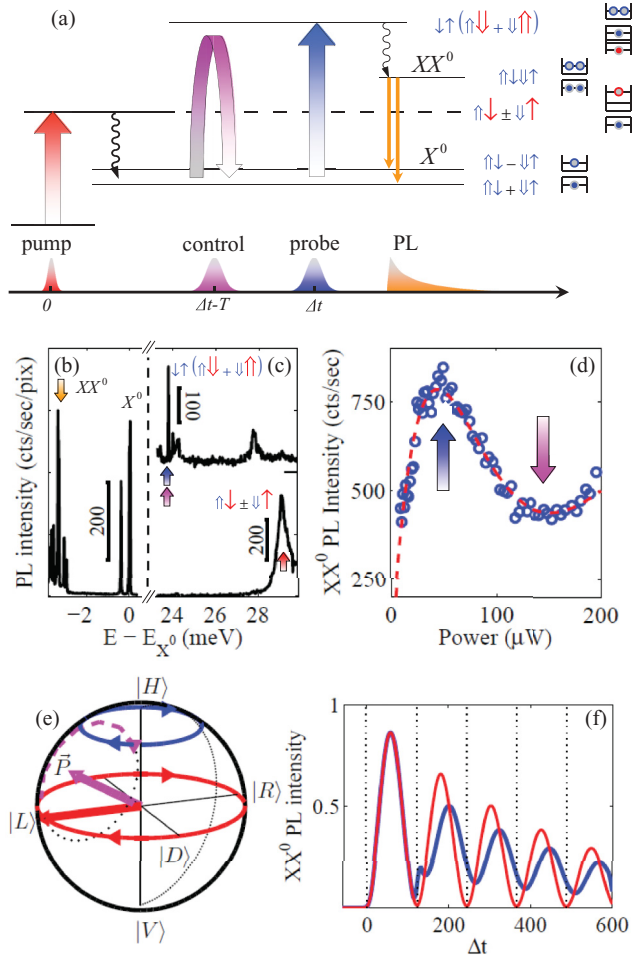


FIG. 1. (Color online) Schematic description of the experiment. (a) The sequence of pulses involved in initialization (pump), control, and readout (probe) of the exciton's spin state. The relevant confined exciton and biexciton levels and their spin wave functions are depicted to the right of each level.  $\uparrow$  ( $\uparrow$ ) denotes the electron (hole) spin state and the short blue (long red) arrow denotes the ground (excited) single carrier state. (b) PL spectrum of the QD. (c) PLE spectra of the exciton (bottom) and biexciton (top). The vertical arrows in (b) and (c) correspond to the optical transitions denoted in (a) by the same colors. (d) The biexciton PL intensity vs. the power of the probe laser [blue arrow in (a) and (c)]. The vertical blue and magenta arrows indicate the laser power which corresponds to pulse area of  $\pi$  (used for the probe) and  $2\pi$  (used for the control) pulses, respectively. The dashed line guides the eye. (e) Bloch sphere representation of the exciton's spin control. (f) The expected absorption of the probe pulse into the biexciton resonance as a function of the delay time ( $\Delta t$ ) between the pump and probe pulses. The blue (red) line describes the absorption with (without) the control pulse as in (e).

the qubit state. For our control operation we use a single  $2\pi$ -area optical pulse, which we tune or slightly detune from a nondegenerate biexcitonic resonance. This  $2\pi$  pulse transfers the excitonic population into itself in a process, which involves photon absorption and stimulated emission. During the process, a relative phase difference is added between the two eigenstates of the exciton spin, resulting in the spin vector

rotation. We show below that the polarization of the control pulse determines the spin rotation axis, and the detuning of the pulse from resonance determines the rotation angle.<sup>8,9</sup> This is markedly different from the situation in which a single charge carrier's spin is controlled<sup>12–16,19–24</sup> or a degenerate resonance is used for the rotation of the exciton spin.<sup>9</sup> In these cases, the polarization is used to distinguish between the degenerate optical transitions, and the polarization degree of freedom is lost, leaving only a *fixed, nontunabile* rotation axis.

The specific biexciton resonance used here for the probe and for the control contains two excitons with antiparallel spins and different spatial symmetries [see Fig. 1(a) and the Supplemental Material<sup>26</sup>]. As a result a polarized pulse in such a resonance couples only to the exciton with the opposite spin state. For example, the *R*-polarized pulse couples to  $|L\rangle$ ,  $H$  to  $|V\rangle$  and  $D$  to  $|\bar{D}\rangle$ , where  $A$  and  $|A\rangle$  are the pulse polarization and the corresponding spin state of the exciton, respectively.<sup>8</sup>

During the pulse, the coupled part of the state acquires a relative geometric phase shift of  $\pi$  radians relative to the uncoupled state.<sup>19,20</sup> On the Bloch sphere, this relative phase acquisition is viewed as a clockwise  $\pi$  rotation of the state's vector about an axis defined by the control pulse polarization direction<sup>9,19,20</sup> (see the Supplemental Material<sup>26</sup>).

Angles of rotations which are different than  $\pi$  are realized by detuning from resonance.<sup>9,19,20</sup> The induced phase shift (or rotation angle) depends on the detuning and the pulse shape. For a hyperbolic secant  $2\pi$  pulse of temporal form  $\alpha \text{sech}(\sigma t) e^{i(E_0 - \Delta)t/\hbar}$ , the phase shift ( $\delta$ ) is given by

$$\delta = \pi - 2 \arctan \left( \frac{\Delta}{\sigma} \right), \quad (1)$$

where  $E_0$  is the resonance energy,  $\sigma$  is the pulse bandwidth, and  $\Delta$  is the detuning from resonance.<sup>9,19,20</sup> Hence, using both polarization and detuning, a universal gate operation is achieved using a *single* pulse.

The sample and the experimental setup are described in the Supplemental Material.<sup>26</sup> The experiment is schematically described in Fig. 1(a), where the relevant energy levels, the resonant optical transitions between them, and the temporal order of the pulses to these resonances are depicted. The particular resonances used in the experiment were identified by PL and PL excitation (PLE) spectroscopy of the QD with one and two resonant lasers,<sup>25</sup> as shown in Figs. 1(b) and 1(c), respectively. The biexciton PL emission intensity versus the intensity of the excitation into the biexciton resonance are depicted in Fig. 1(d), where the intensities which correspond to a  $\pi$  and a  $2\pi$  pulse, used for the probe and for the control, respectively, are marked. We note that under the  $2\pi$ -pulse excitation the signal does not go to zero. This results from the short lifetime of the resonance used for the control pulse. The resonantly excited hole decays within 20 ps to a lower, metastable biexcitonic state.<sup>27,28</sup> As a result, part of the excitonic population is lost to the biexciton during the 9-ps  $2\pi$  pulse. The biexcitonic population returns incoherently by spontaneous radiative recombination within about 600 ps to the exciton state. Since we probe the exciton only 122 ps after the control pulse the effect of the incoherent population is a very small decrease in the visibility.

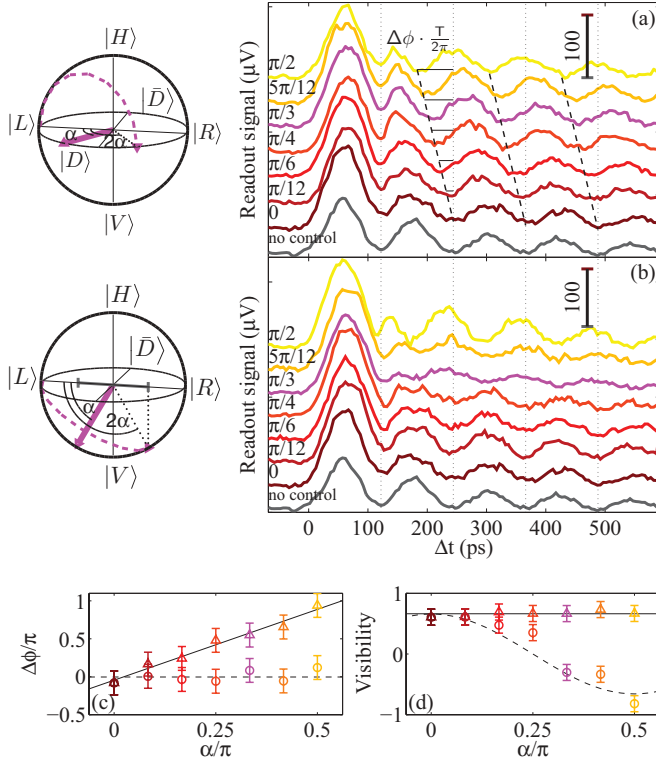


FIG. 2. (Color online) Biexciton PL intensity (lock-in detected with the probe pulse) vs  $\Delta t$  for various control pulse polarizations given by  $\vec{P}(\theta, \phi) = \vec{P}(\frac{\pi}{2}, \pi + \alpha)$  in (a) and  $\vec{P}(\theta, \phi) = \vec{P}(\frac{\pi}{2} + \alpha, \pi)$  in (b), where  $\alpha$  varies from 0 ( $L$  polarization) to  $\pi/2$  [ $D$  polarization in (a) and  $V$  polarization in (b)]. The control pulse is one period of oscillation before the probe. The lowest curve in (a) and in (b) describes the measurement without the control pulse, and it is used for normalization. The rotation of the exciton's spin induced by the polarized control pulse is schematically described as a trajectory on the Bloch spheres to the left of each panel. (c) [(d)] Symbols: The phase shifts (normalized visibilities) of the exciton spin precession induced by the control pulse vs  $\alpha$ . The triangles' (circles') colors match the colors in (a) [(b)]. The solid (dashed) lines are best fits to the experimental points in (a) [(b)].

In Fig. 1(e), the exciton's spin Bloch sphere is used to schematically describe the optical control. The red circle on the sphere surface in Fig. 1(e) describes the precession of the exciton spin after initialization by an  $L$ -polarized pulse, represented by a thick red arrow. The thick magenta arrow in Fig. 1(e) describes the direction of the polarization  $\vec{P}(\theta, \phi)$  of the control  $2\pi$  pulse, where the polar ( $\theta$ ) and azimuthal ( $\phi$ ) angles are defined in the figure. The dashed magenta line describes the rotation of the exciton state during the control pulse, and the blue line describes the precession of the exciton state *after* the control pulse ends. The curves in Fig. 1(f) describe the magnitude of the absorption of the probe pulse versus the time difference ( $\Delta t$ ) between the generation (pump) and readout (probe) pulses. The red and blue curve correspond to a measurement without the control pulse and with it, respectively. The control pulse is timed exactly one precession period *before* the probe pulse. Thus, the control action is detected a period after it occurs.

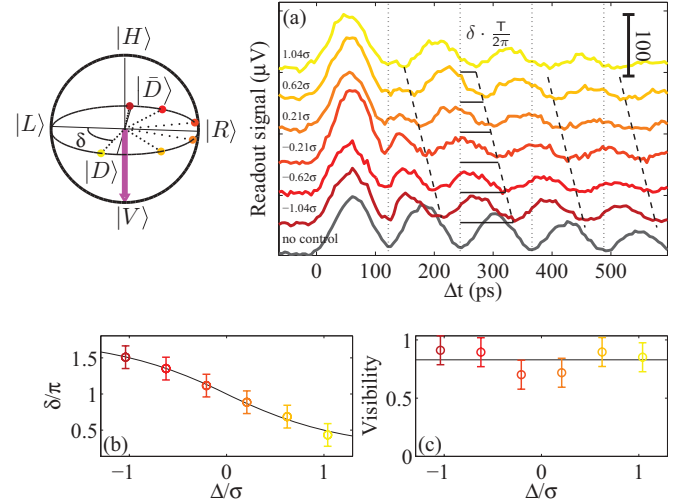


FIG. 3. (Color online) (a) Biexciton PL intensity vs  $\Delta t$  for a  $V$ -polarized variably detuned control pulse. The rotation of the exciton's spin induced by the control pulse is schematically described as a trajectory on the Bloch sphere to the left. (b) [(c)] Circles: The phase shifts (normalized visibilities) of the exciton spin vs the detuning  $\delta$  in units of the pulse bandwidth  $\sigma$ . The solid lines are best fits using Eq. (1) in (b) and to a constant dependence on  $\delta/\sigma$  in (c).

In Figs. 2 and 3 we display three series of experiments which demonstrate our ability to perform universal gate operations on the exciton state using a *single* optical pulse. In these experiments, as in Fig. 1, the exciton is always photogenerated in its  $|L\rangle$  coherent state by an  $L$ -polarized pulse. The probe pulse, which in these experiments is delayed continuously relative to the pump, is also  $L$  polarized, thus projecting the exciton state onto the  $|R\rangle$  state. The lowest, black solid line in each figure describes for comparison the two-pulse experiment in the absence of a control pulse, in which the precession of an  $|L\rangle$  photogenerated exciton is probed by the delayed  $L$ -polarized probe pulse.<sup>8</sup>

The control  $2\pi$  pulse is always launched one precession period ( $T = 122$  ps) *before* the probe pulse. Thus its influence on the probe signal is noticed only if the control acts after the pump, i.e., at  $\Delta t > T$ .

In Fig. 2, the first two sets of experiments are presented. Here, the control pulse is tuned to resonance and its polarization is given by  $\vec{P}(\theta, \phi) = \vec{P}(\pi/2, \pi + \alpha)$  and  $\vec{P}(\theta, \phi) = \vec{P}(\pi/2 + \alpha, \pi)$  in Figs. 2(a) and 2(b), respectively. The angle  $\alpha$  spans seven equally spaced values from 0 ( $L$  polarization) to  $\pi/2$  [ $D$  and  $V$  polarizations in Figs. 2(a) and 2(b), respectively], as denoted to the left of each curve. The situation is schematically described on the Bloch spheres to the left of Figs. 2(a) and 2(b). The control applies  $\pi$  rotation on the exciton state vector around the polarization direction  $\vec{P}$ . The trajectory on the surface of the Bloch sphere represents this rotation applied to the initial  $|L\rangle$  state. In Fig. 2(a) the rotation always leaves the exciton state on the equator plane while imparting a phase shift which amounts to twice the angle  $\alpha$  [dashed line in Fig. 2(a)]. In Fig. 2(b) the rotations leave the exciton phase fixed while varying the state projection on the equator (visibility) as  $\cos(2\alpha)$ .

In Figs. 2(c) and 2(d) the measured phase shift of the exciton state and its visibility are displayed, respectively, as a function of  $\alpha$ . As expected from the geometrical description, for the rotations in Fig. 2(a), the visibility does not vary with  $\alpha$  while the phase shift varies linearly from 0 to  $\pi$  as  $\alpha$  varies from 0 to  $\pi/2$  (best fits are described by the solid lines). For the rotations in Fig. 2(b), the visibility does vary as  $\cos(2\alpha)$ , while the phase shift remains unchanged (best fits are described by the dashed lines).

In order to complete the demonstration of single pulse control, in Fig. 3(a) we present a series of measurements in which the control pulse polarization is fixed at  $\vec{P}(\theta, \phi) = \vec{P}(\pi, \pi)$  ( $V$  polarization) while we vary the pulse detuning from resonance. The situation is schematically described on the Bloch sphere to the left [Fig. 3(a)], which shows the rotations the control pulse imparts to the exciton state. Here, the rotations are achieved through variations in the angle by which the pulse rotates the state around the polarization direction. As is shown in the figure, the exciton state remains on the equator, while it acquires an additional phase of  $\delta$  [Eq. (1)] to its azimuthal angle  $\phi$ . In Figs. 3(c) and 3(d) the measured phase shift of the exciton state and its visibility, respectively, are displayed as functions of the detuning  $\Delta$  measured in units of the laser bandwidth  $\sigma$ . While the visibility does not vary

with the detuning,  $\delta$  varies from approximately  $3\pi/2$  to  $\pi/2$  as  $\Delta/\sigma$  varies from  $-1$  to  $1$ .

In summary, we demonstrate complete control of the spin state of an exciton in a QD using a single  $2\pi$ -area laser pulse, resonant with, or slightly detuned from, a nondegenerate biexciton state. Any desired rotation of the spin state is achieved by controlling three degrees of freedom. The first two are the angles which define the rotation axis around which the exciton spin state is rotated during the short control pulse. These angles are fully determined by the pulse polarization direction. The third is an arbitrary angle of rotation, which is fully determined by the detuning from the biexciton resonance. The method presented here is not unique to excitons in QDs,<sup>29</sup> it is applicable to other qubit systems as well, including, but not limited to, nitrogen-vacancy centers in diamonds.<sup>30</sup> The only requirement is an optical transition to a nondegenerate excited resonance.

The support of the US-Israel Binational Science Foundation (BSF), the Israeli Science Foundation (ISF), the Ministry of Science and Technology (MOST), Eranet Nano Science Consortium, and the Technion's RBNI are gratefully acknowledged.

\*dg@physics.technion.ac.il

<sup>1</sup>A. Barenco, C. H. Bennett, R. Cleve, D. P. DiVincenzo, N. Margolus, P. Shor, T. Sleator, J. A. Smolin, and H. Weinfurter, *Phys. Rev. A* **52**, 3457 (1995).

<sup>2</sup>D. P. DiVincenzo, *Fortschr. Phys.* **48**, 771 (2000).

<sup>3</sup>T. D. Ladd, F. Jelezko, R. Laflamme, Y. Nakamura, C. Monroe, and J. L. O'Brien, *Nature (London)* **464**, 45 (2010).

<sup>4</sup>E. Poem, Y. Kodriano, C. Tradonsky, N. H. Lindner, B. D. Gerardot, P. M. Petroff, and D. Gershoni, *Nat. Phys.* **6**, 993 (2010).

<sup>5</sup>A. J. Ramsay, S. J. Boyle, R. S. Kolodka, J. B. B. Oliveira, J. Skiba-Szymanska, H. Y. Liu, M. Hopkinson, A. M. Fox, and M. S. Skolnick, *Phys. Rev. Lett.* **100**, 197401 (2008).

<sup>6</sup>A. Boyer de la Giroday, A. J. Bennett, M. A. Pooley, R. M. Stevenson, N. Sköld, R. B. Patel, I. Farrer, D. A. Ritchie, and A. J. Shields, *Phys. Rev. B* **82**, 241301 (2010).

<sup>7</sup>S. Michaelis de Vasconcellos, S. Gordon, M. Bichler, T. Meier, and A. Zrenner, *Nat. Photonics* **4**, 545 (2010).

<sup>8</sup>Y. Benny, S. Khatsevich, Y. Kodriano, E. Poem, R. Presman, D. Galushko, P. M. Petroff, and D. Gershoni, *Phys. Rev. Lett.* **106**, 040504 (2011).

<sup>9</sup>E. Poem, O. Kenneth, Y. Kodriano, Y. Benny, S. Khatsevich, J. E. Avron, and D. Gershoni, *Phys. Rev. Lett.* **107**, 087401 (2011).

<sup>10</sup>D. Loss and D. P. DiVincenzo, *Phys. Rev. A* **57**, 120 (1998).

<sup>11</sup>A. Imamoğlu, D. D. Awschalom, G. Burkard, D. P. DiVincenzo, D. Loss, M. Sherwin, and A. Small, *Phys. Rev. Lett.* **83**, 4204 (1999).

<sup>12</sup>J. R. Petta, A. C. Johnson, J. M. Taylor, E. A. Laird, A. Yacoby, M. D. Lukin, C. M. Marcus, M. P. Hanson, and A. C. Gossard, *Science* **309**, 2180 (2005).

<sup>13</sup>F. H. L. Koppens, C. Buizert, K. J. Tielrooij, I. T. Vink, K. C. Nowack, T. Meunier, L. P. Kouwenhoven, and L. M. K. Vander-sypen, *Nature (London)* **442**, 766 (2006).

<sup>14</sup>J. Berezovsky, M. H. Mikkelsen, N. G. Stoltz, L. A. Coldren, and D. D. Awschalom, *Science* **320**, 349 (2008).

<sup>15</sup>D. Press, T. D. Ladd, B. Zhang, and Y. Yamamoto, *Nature (London)* **456**, 218 (2008).

<sup>16</sup>K. De Greve, P. L. McMahon, D. Press, T. D. Ladd, D. Bisping, C. Schneider, M. Kamp, L. Worschech, S. Höfling, A. Forchel, and Y. Yamamoto, *Nat. Phys.* **7**, 872 (2011).

<sup>17</sup>A. Greilich, S. G. Carter, D. Kim, A. S. Bracker, and D. Gammon, *Nat. Photonics* **5**, 702 (2011).

<sup>18</sup>T. M. Godden, J. H. Quilter, A. J. Ramsay, Y. Wu, P. Brereton, S. J. Boyle, I. J. Luxmoore, J. Puebla-Nunez, A. M. Fox, and M. S. Skolnick, *Phys. Rev. Lett.* **108**, 017402 (2012).

<sup>19</sup>S. E. Economou, L. J. Sham, Y. Wu, and D. G. Steel, *Phys. Rev. B* **74**, 205415 (2006).

<sup>20</sup>S. E. Economou and T. L. Reinecke, *Phys. Rev. Lett.* **99**, 217401 (2007).

<sup>21</sup>Y. Wu, E. D. Kim, X. Xu, J. Cheng, D. G. Steel, A. S. Bracker, D. Gammon, S. E. Economou, and L. J. Sham, *Phys. Rev. Lett.* **99**, 097402 (2007).

<sup>22</sup>A. Greilich, S. E. Economou, S. Spatzek, D. R. Yakovlev, D. Reuter, A. D. Wieck, T. L. Reinecke, and M. Bayer, *Nat. Phys.* **5**, 262 (2009).

<sup>23</sup>E. D. Kim, K. Truex, X. Xu, B. Sun, D. G. Steel, A. S. Bracker, D. Gammon, and L. J. Sham, *Phys. Rev. Lett.* **104**, 167401 (2010).

<sup>24</sup>D. Kim, S. G. Carter, A. Greilich, A. S. Bracker, and D. Gammon, *Nat. Phys.* **7**, 223 (2011).

<sup>25</sup>Y. Benny, Y. Kodriano, E. Poem, S. Khatsevich, D. Gershoni, and P. M. Petroff, *Phys. Rev. B* **84**, 075473 (2011).

<sup>26</sup>See Supplemental Material at <http://link.aps.org/supplemental/10.1103/PhysRevB.85.241304> for detailed description of the experimental setup, the data reduction procedures and the theory pertaining to the universal gate control.

<sup>27</sup>E. Poem, Y. Kodriano, C. Tradonsky, B. D. Gerardot, P. M. Petroff, and D. Gershoni, [Phys. Rev. B \*\*81\*\*, 085306 \(2010\)](#).

<sup>28</sup>Y. Kodriano, E. Poem, N. H. Lindner, C. Tradonsky, B. D. Gerardot, P. M. Petroff, J. E. Avron, and D. Gershoni, [Phys. Rev. B \*\*82\*\*, 155329 \(2010\)](#).

<sup>29</sup>G. Ramon, U. Mizrahi, N. Akopian, S. Braitbart, D. Gershoni, T. L. Reinecke, B. D. Gerardot, and P. M. Petroff, [Phys. Rev. B \*\*73\*\*, 205330 \(2006\)](#).

<sup>30</sup>B. B. Buckley, G. D. Fuchs, L. C. Bassett, and D. D. Awschalom, [Science \*\*330\*\*, 1212 \(2010\)](#).